Table I. A patient with psoriasis versus a patient with GID*

Measures	Patient with psoriasis, mean (SD)	Patient with GID, mean (SD)	$t_{(289)}$	*P*
Caretaking disposition	2.8 (0.8)	3.1 (0.8)	−4.463	<.0001
Caretaking avoidance	4.0 (1.5)	3.3 (1.5)	7.288	<.0001
Disease origin attribution				
Genetic factors	3.2 (0.9)	2.9 (0.7)	4.901	<.0001
Personal responsibility	2.3 (0.8)	2.8 (0.8)	−6.942	<.0001
Chance	2.1 (1.0)	2.0 (0.9)	1.409	.160
Anticipated stigma endorsement	11.6 (2.2)	10.2 (2.6)	7.696	<.0001

GID, Gastrointestinal disease; *SD*, standard deviation.
*Mean (SD) scores obtained by medical students on stigma-related variables for a patient with psoriasis and a patient with GID.

Table II. An ingroup versus an outgroup patient with psoriasis*

Measures	Ingroup patient with psoriasis, mean (SD)	Outgroup patient with psoriasis, mean (SD)	$t_{(288)}$	*P*
Caretaking disposition	2.9 (0.9)	2.8 (0.9)	0.721	.471
Caretaking avoidance	3.7 (1.5)	4.2 (1.5)	−2.046	.042
Disease origin attribution				
Genetic factors	3.3 (0.8)	3.1 (0.9)	1.726	.085
Personal responsibility	2.2 (0.8)	2.5 (0.9)	−1.907	.057
Chance	2.3 (1.1)	2.0 (0.9)	1.830	.068
Anticipated stigma endorsement	12.3 (2.1)	11 (2.1)	4.954	<.0001

GID, Gastrointestinal disease; *SD*, standard deviation.
*Mean (SD) scores obtained by medical students on stigma-related variables for an ingroup and an outgroup patient with psoriasis.

Table III. An ingroup versus an outgroup patient with GID*

Measures	Ingroup patient with GID, mean (SD)	Outgroup patient with GID, mean (SD)	$t_{(288)}$	*P*
Caretaking disposition	3.1 (0.8)	3.0 (0.8)	−0.627	.531
Caretaking avoidance	3.3 (1.3)	3.2 (1.1)	−1.017	.311
Disease origin attribution				
Genetic factors	2.9 (0.7)	2.9 (0.8)	0.818	.414
Personal responsibility	2.8 (0.8)	2.7 (0.8)	−1.063	.289
Chance	2.0 (0.9)	2.1 (1.0)	0.712	.477
Anticipated stigma endorsement	10.3 (2.5)	10.2 (2.7)	−0.402	.688

GID, Gastrointestinal disease; *SD*, standard deviation.
*Mean (SD) scores obtained by medical students on stigma-related variables for an ingroup and an outgroup patient with GID.

E-mail: edita.fino@unibo.it

REFERENCES

1. van Brakel WH, Cataldo J, Grover S, et al. Out of the silos: identifying cross-cutting features of health-related stigma to advance measurement and intervention. *BMC Med*. 2019;17:13.
2. Stang AL, Earnshaw VA, Logie CH, et al. The Health Stigma and Discrimination Framework: a global, crosscutting framework to inform research, intervention development, and policy on health-related stigmas. *BMC Med*. 2019;17:31.
3. Jackson-Best F, Edwards N. Stigma and intersectionality: a systematic review of systematic reviews across HIV/AIDS, mental illness, and physical disability. *BMC Public Health*. 2018;18:919.
4. Pearl RL, Wan MT, Takeshita J, Gelfand JM. Stigmatizing attitudes toward persons with psoriasis among laypersons and medical students. *J Am Acad Dermatol*. 2019;80:1556-1563.
5. Pescosolido BA, Martin JK. The stigma complex. *Annu Rev Sociol*. 2015;41:87-116.

https://doi.org/10.1016/j.jaad.2020.06.060

Color Doppler ultrasonographic evaluation of management of papulopustular rosacea

To the Editor: Rosacea is a chronic inflammatory disorder that commonly affects the face and presents several phenotypes; however, to date, there are still gaps in the understanding of rosacea pathophysiology.[1] Particularly, in papulopustular rosacea lesions (PPR), topical ivermectin and metronidazole

Table I. Baseline color Doppler ultrasonography features of healthy control individuals and patients with PPR

Characteristics	Control individuals (n = 10)	Baseline (n = 27)	*P* value
Right cheek			
Dermal thickness, mm, mean ± SD	1.6 ± 0.2	1.6 ± 0.4	.95
Dermal echogenicity, n (%)			
Hyperechoic	3 (30.0)	6 (22.2)	.30
Hypoechoic	**0 (0)**	**21 (77.8)**	**<.01**
Mix (hyperechoic and hypoechoic)	**7 (70.0)**	**0 (0)**	**<.01**
Dermis-subcutis hypervascularity, n (%)			
Absent	**6 (60.0)**	**1 (3.7)**	**<.01**
Present	**4 (40.0)**	**26 (96.3)**	**<.01**
Thickness of vessels, mm, mean ± SD	0.7 ± 0.3	1.0 ± 0.2	.15
Peak systolic velocity of arterial vessels, cm/s, mean ± SD	4.2 ± 1.5	6.3 ± 2.3	.11
Nasal region			
Dermal thickness, mm, mean ± SD	1.5 ± 0.3	1.8 ± 0.4	.07
Dermal echogenicity, n (%)			
Hyperechoic	**1 (10.0)**	**0 (0)**	**.04**
Hypoechoic	8 (80.0)	27 (100)	.08
Mix (hyperechoic and hypoechoic)	**1 (10.0)**	**0 (0)**	**.04**
Dermis-subcutis hypervascularity, n (%)			
Absent	**10 (100)**	**1 (3.7)**	**<.01**
Present	**0 (0)**	**26 (96.3)**	**<.01**
Thickness of vessels, mm, mean ± SD	—	0.7 ± 0.4	—
Peak systolic velocity of arterial vessels, cm/s, mean ± SD	—	6.4 ± 4.0	—
Alar nasal cartilages			
Thickness, mm, mean ± SD	1.7 ± 0.3	2.0 ± 0.6	.11
Hypervascularity, n (%)			
Absent	7 (70)	13 (48.1)	.11
Present	3 (30)	14 (51.9)	.11
Thickness of vessels, mm, mean ± SD	0.9 ± 0.2	0.8 ± 0.4	.41
Peak systolic velocity of arterial vessels, cm/s, mean ± SD	4	6.8 ± 3.2	.81

Significant Values are indicated by bold text.
PPR, Papulopustular rosacea; *SD*, standard deviation.

are first-line treatments.[1,2] Color Doppler ultrasonography (CDU) is a noninvasive imaging technique that can support a broad spectrum of dermatologic conditions.[3]

A double-blind randomized controlled clinical trial was conducted in patients with rosacea from March to September 2018. The aim of this study was to evaluate the ultrasonographic findings in patients with PPR rosacea treated with topical ivermectin and metronidazole. The study was approved by the institutional review board (no. 472920), and the clinical trial number is NCT24435875.

The CDU examination recorded the thickness and vascularity of the dermis and subcutis of the right cheek and nasal tip as well as at the alar cartilage in patients (baseline and at the 12-week follow-up) and 10 healthy control individuals. Statistical significance was assessed at a *P* value of less than .05. More details on the methodology, inclusion and exclusion criteria, and statistics are described in the supplemental materials (available via Mendeley at https://doi.org/10.17632/bn89h9kkn3.1).

Twenty-seven patients entered the study, and 23 completed the follow-up. The clinical and ultrasonographic characteristics of the patients and healthy control individuals are described in Table I and Supplemental Tables I to III (available via Mendeley at https://doi.org/10.17632/bn89h9kkn3.1).

At baseline, patients with PPR presented a significantly higher dermal and subcutis vascularity in the right cheek and nasal region and higher hypoechogenicity of the dermis of the cheek ($P < .01$). At the nasal region, the dermis was hypoechoic or heterogeneous in both groups; however, a slight raising or undulation of the epidermis was noted only in PPR cases. Overall, 96.3% of patients with PPR presented with dermal and subcutis facial hypervascularity, and 51.9% showed hypervascularization of the alar nasal cartilages. Regardless of the type of treatment, none of the ultrasonographic parameters showed

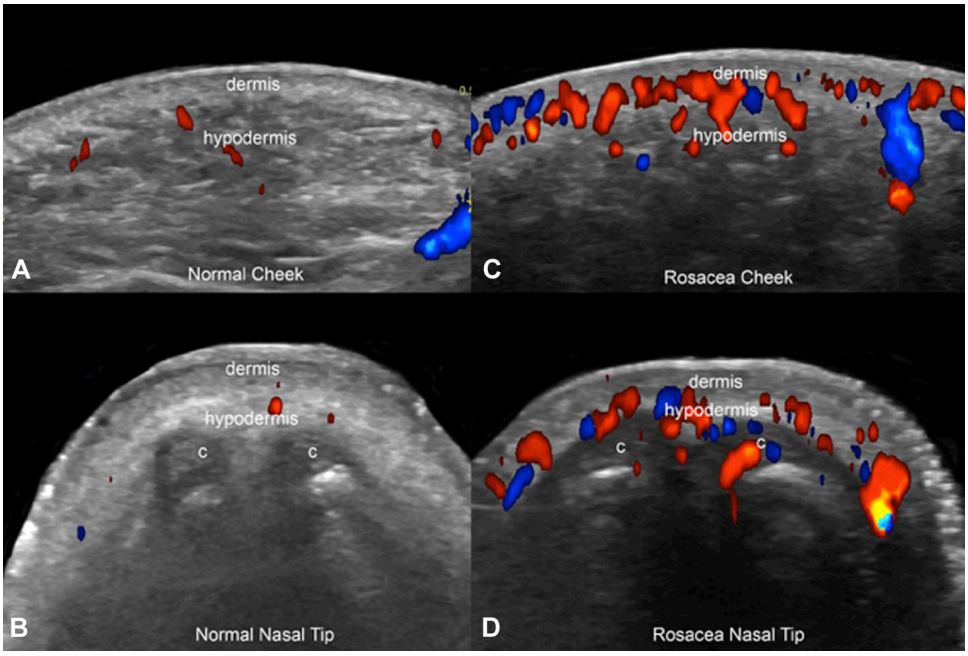

Fig 1. Color Doppler ultrasonographic comparative views of (**A**, **B**) healthy control individuals and (**C**, **D**) patients with rosacea at the (**A**, **C**) right check and (**B**, **D**) nasal tip (transverse views). Notice the dermal and hypodermal hypervascularity at the cheek in the rosacea. There is also increased dermal and hypodermal vascularity as well as hypervascularity of the alar cartilage at the nasal tip in rosacea. *c*, Alar cartilage.

significant changes at the follow-up. Additionally, no association was found between the clinical variables and the presence of vascularity within the nasal cartilages (Fig 1).

The clinical number of inflammatory lesions significantly decreased in both groups; however, the investigator's global assessment score significantly decreased only for metronidazole.

Despite the high prevalence of rosacea worldwide, we found only 1 reference on ultrasonography of rosacea based on personal experience.[4] In our PPR sample, even though there was a clinical improvement, there were anatomic alterations of deeper layers and a lack of significant ultrasonographic changes after the administration of both topical treatments. This means that rosacea is not only a superficial cutaneous condition and that clinical evaluation alone can underestimate the degree of the inflammatory process. In addition, topical agents may be insufficient to treat the involvement of deeper layers.

Limitations of our study are the small sample and the impossibility of detecting ultrasonographically alterations of less than 0.1 mm.[3]

Subclinical ultrasonographic alterations and activity have been found in other inflammatory diseases such as hidradenitis suppurativa.[5] In rosacea, this may explain the frequent relapses and rhinophyma. In conclusion, regardless of the type of treatment, ultrasonography shows evidence of deeper inflammation in PPR, and this should require further research.

Roberto Bustos, MD,[a] Andrea Cortes, MD,[a] Maria Elena McNab, MD,[a] Eliseo Fuentes, MS,[b] Ariel Castro, MSc,[c] and Ximena Wortsman, MD[a,d]

From the Department of Dermatology, Faculty of Medicine, Universidad de Chile[a]; School of Medicine, Universidad de Chile[b]; Office for Clinical Research Support, Hospital Clinico Universidad de Chile[c]; and the Institute for Diagnostic Imaging and Research of the Skin and Soft Tissues, Santiago, Chile.[d]

Funding sources: None.

Conflicts of interest: None disclosed.

IRB approval status: Reviewed and approved by the Hospital Clínico Universidad de Chile IRB (no. 472920).

Reprints are not available from the authors.

Correspondence to: Roberto Bustos, MD, Department of Dermatology, Hospital Clinico, Universidad de Chile, Santos Dumont 999, Independencia, Santiago, Chile

E-mail: robertobustos@med.uchile.cl

REFERENCES

1. Gallo RL, Granstein RD, Kang S, et al. Standard classification and pathophysiology of rosacea: the 2017 update by the National Rosacea Society Expert Committee. *J Am Acad Dermatol*. 2018;78(1):148-155.
2. Tan J, Berg M. Rosacea: current state of epidemiology. *J Am Acad Dermatol*. 2013;69(6 Suppl 1):S27-S35.
3. Wortsman X. Common applications of dermatologic sonography. *J Ultrasound Med*. 2012;31(1):97-111.
4. Wortsman X. Color Doppler ultrasound. In: Kaminsky A, Piquero-Martin J, Herane MI, Diez de Medina J, Florez White M, Iberian-Latin American Acne and Rosacea Study Group GILEAR, eds. *Rosacea: A Comprehensive View*. 1st ed. 2020:259-266.
5. Wortsman X, Moreno C, Soto R, Arellano J, Pezo C, Wortsman J. Ultrasound in-depth characterization and staging of hidradenitis suppurativa. *Dermatol Surg*. 2013;39:1835-1842.

https://doi.org/10.1016/j.jaad.2020.06.068

A deep learning algorithm to detect the presence of basal cell carcinoma on Mohs micrographic surgery frozen sections

To the Editor: Nonmelanoma skin cancer represents the most common cancer in the United States with more than 5.4 million cases annually, of which 8 in 10 are basal cell carcinomas (BCCs).[1] Mohs micrographic surgery (MMS) treats BCCs by providing margin control. The process of accurate and complete interpretation of frozen section slides would benefit from the presence of a second reader. We seek to apply deep learning to MMS by developing an algorithm to aid the surgeon in detecting BCC on frozen sections.

We retrospectively selected 75 cases that had positive findings for BCC on MMS and 25 cases that initially had biopsy-proven BCC but had negative findings for tumor on the first stage of MMS among all MMS cases with a biopsy-confirmed diagnosis of BCC and available frozen section slides performed at a single academic center from 2011 to 2018. Digital images of each frozen section were taken at ×2 magnification with a 2-megapixel Olympus (Tokyo, Japan) DP20-5 digital camera. Each ×2 image was independently assigned as positive or negative for BCC. The data were randomly partitioned into 60% training, 20% validation, and 20% test set at the case level. The images were preprocessed via resizing, normalization, and standard data augmentation. A class-balanced data set was fed through the 2-dimensional residual nets (ResNet)[2] pretrained with ImageNet (Stanford Vision Lab, Stanford University, Princeton University). After random hyperparameter search, we arrived at a ResNet-50 with Adam optimizer and learning rate of 0.001 with a dropout of 0.2.

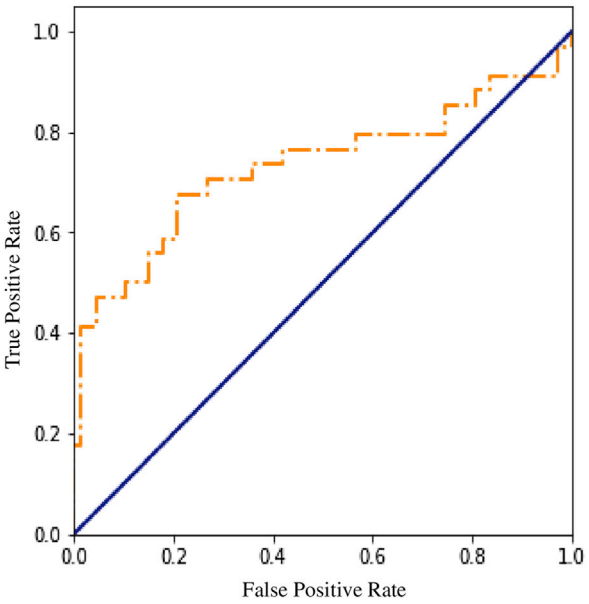

Fig 1. Receiver operating characteristic curve. The curve shows the overall performance of the deep learning algorithm, showing the tradeoff between sensitivity and specificity. The area under the curve is 0.753.

The final model evaluated on the holdout test set achieved an area under the receiver operating characteristic curve of 0.753 (Fig 1). Representative sensitivity/specificity tradeoff values were a sensitivity of 70.6% at specificity of 79.1%. The most common source of false positives was dense aggregates of inflammatory cells, and the most common source of false negatives was small aggregates of tumor cells in relation to the specimen size (Fig 2).

Our algorithm has several key strengths. First, the model consistently analyzes an image through the neural network parameters without emotional bias. Second, it can conduct a detailed image analysis at the pixel level, limited only by the inherent noise of the microscope and camera. The approaches to image analysis by the Mohs surgeon and algorithm differ fundamentally, and consequently, their combined efforts provide increased accuracy of BCC detection, as reflected in the concept of ensemble learning.[3] Finally, the algorithm serves as a safety mechanism to help the surgeon avoid missing residual tumor.

Our model has several notable limitations. Most importantly, our pilot algorithm is limited by the small sample size. A larger, more diverse data set is needed to achieve higher area under the curve and